Available online at www.eccomasproceedia.org
Eccomas Proceedia COMPDYN (2017) 1545-1557

ECCOMAS
Proceedia

COMPDYN 2017
6th ECCOMAS Thematic Conference on
Computational Methods in Structural Dynamics and Earthquake Engineering
M. Papadrakakis, M. Fragiadakis (eds.)
Rhodes Island, Greece, 15–17 June 2017

RINTC PROJECT: ASSESSING THE (IMPLICIT) SEISMIC RISK OF CODE-CONFORMING STRUCTURES IN ITALY*

Iunio Iervolino,[1] Andrea Spillatura,[2] and Paolo Bazzurro[2]

[1]Dip. di Strutture per l'Ingegneria e l'Architettura, Università degli Studi di Napoli Federico II
via Claudio 21, 80125, Naples, Italy.
e-mail: iunio.iervolino@unina.it

[2]University School for Advanced Studies IUSS Pavia
Palazzo del Broletto – Piazza della Vittoria 15, 27100, Pavia, Italy.
e-mail: andrea.spillatura@umeschool.it; paolo.bazzurro@iusspavia.it

Keywords: Performance-based earthquake engineering, Reliability, Failure, Damage, Hazard.

Abstract. *RINTC, which started in 2015, is a joint project of ReLUIS and EUCENTRE, two centers of competence for seismic risk assessment of the Italian civil protection. The goal of the project, which is still ongoing, is to assess in an explicit manner the seismic risk of structures designed according to the code currently enforced in Italy. To this aim five structural typologies were considered: masonry, reinforced concrete, pre-cast reinforced concrete, steel, and seismically isolated buildings. In the framework of the project, multiple archetype structures have been designed for each typology according to standard practice at five sites across Italy, spanning a wide range of seismic hazard levels. The seismic vulnerability of the designed structures was assessed by subjecting 3D computer models to multi-stripe non-linear dynamic analysis. Integration of the probabilistic hazard and probabilistic vulnerability (i.e., fragility) yielded the annual failure rate, in terms of onset of non-structural damage and collapse, of each of the structures. Risk assessment takes into consideration record-to-record variability of non-structural response and, for selected cases, structural modeling uncertainty. Results preliminarily show that, for each structural typology, the collapse risk tends to increase with the hazard of the site and that risk is not uniform across typologies.*

Peer-review under responsibility of the organizing committee of COMPDYN 2017.
doi: 10.7712/120117.5512.17282

* Revised post-conference on June 2017.

1 INTRODUCTION

The current Italian seismic code [1], the *Norme Tecniche per le Costruzioni* (NTC08 hereafter), allows engineers to design seismic resistant structures with respect to the onset of a number of pre-defined performance targets, or *limit states*. As in many modern (advanced) seismic codes, the safety margins against exceedance of these limit states are not directly controlled during design. In other words, the probability that the structure, during its design life, fails to meet the performance objectives is not known. In fact, design is carried out such that the structure is expected to withstand relatively rare ground motion intensities at the site of the construction computed according to probabilistic seismic hazard analysis [2]. In particular, design seismic actions (i.e., elastic response spectrum ordinates) are those corresponding to a specified the return period, T_R (i.e., they are exceeded at the site of the construction, on average, once in a number of years corresponding to T_R). For example, an ordinary structure has to be designed for the life-safety limit state considering ground motions with return period of 475 years (i.e., probability of exceedance of 10% in 50 years). Although design seismic actions have a probabilistic definition, the resulting failure probability is, however, not explicitly controlled because of two main issues: (i) NTC08 prescribes design safety margins on seismic structural capacity (e.g., material design values, capacity design, minimum member size, etc.) that are independent of the site hazard; (ii) there is no guarantee that, because of record-to-record variability of seismic response, either the structure will not fail for ground motions of intensity lower than the design one or that it will fail for intensity larger than the design one. Issue (i) tends to lower the failure probability with respect to the exceedance probability of the ground motion intensity used for design, while issue (ii) tends to increase it. The effect of these competing factors on the reliability of the structure is not explicitly controlled by the design engineer. Moreover, because design procedures may be different for different structural typologies or multiple design options are available for the same structural type, the code does not warrant that different structures designed for the same site, or similar structures at different sites, have the same failure probability with respect to the same performance target. Knowledge of these failure probabilities would form a sound basis for further understanding the seismic safety level of code-conforming structures. This motivated the RINTC project, which is a nationwide research program funded by the Italian civil protection to ReLUIS (the Italian network of earthquake engineering university labs; http://www.reluis.it) and EUCENTRE (the European Centre for Training and Research in Earthquake Engineering; http://www.eucentre.it). RINTC is its third year, and its preliminary results in terms of failure probability of code-conforming structure are summarized herein.

For the purposes of the project, five Italian sites were considered (Figure 1) in such a way to span a wide range of seismic hazard levels (Table 1) within the country. Furthermore, for each site, two local soil conditions are considered, A- and C-type according to Eurocode 8 [3] classification. Five structural typologies of buildings were studied: un-reinforced masonry, cast-in-place reinforced concrete, pre-cast reinforced concrete, steel, base-isolated. The structures belonging to different typologies were designed for the same sites. 3D non-linear structural models were developed for the designed structures, and their seismic performance was evaluated via non-linear dynamic analysis. This allowed obtaining a probabilistic characterization of the seismic response for all possible levels of shaking at the site of interest. The latter, coupled with probabilistic seismic hazard, permitted the calculation for the designed structures of the annual failure rates (that are numerically almost identical to annual probabilities), which in turn enabled an assessment of the seismic safety and a reliability comparison across structural typologies and sites. The failure probability was evaluated with respect to structural collapse and onset of non-structural damage; however, herein only collapse

rates are presented. In the following the main results (that are preliminary, because the project is still ongoing) are presented. However, the interested reader can find more in-depth discussions in [4] and in other companion papers (referenced in the following) presented in this same conference that provide design, modeling, and analysis details for each structural typology investigated.

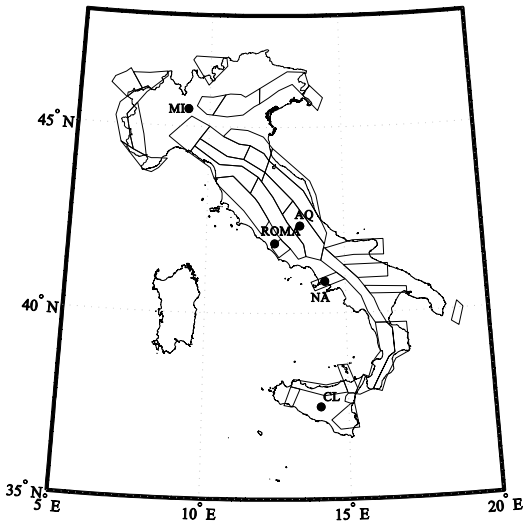

Figure 1: Location of the considered sites and seismic source model at the basis of the official Italian hazard map used to determine design seismic actions [2].

Site	Lon.	Lat.	PGA $\left(T_R = 475yr\right)$ A-type soil [g]
Milano (MI)	9.19	45.47	0.05
Caltanissetta (CL)	14.06	37.48	0.08
Roma (RM)	12.48	41.87	0.12
Napoli (NA)	14.27	40.85	0.17
L'Aquila (AQ)	13.40	42.35	0.26

Table 1: Site coordinates and design peak ground acceleration (PGA) on A-type soil for life-safety limit state.

The reminder of the paper presents first the methodology to compute the failure probabilities, followed by the case-study structures, and by a discussion about seismic hazard and the selection of ground motions for non-linear dynamic analysis. The article ends with the presentation of the results of the first two years of the project and with preliminary conclusions.

2 METHODOLOGY

The final results of the project are represented by the annual failure rates of the considered code-conforming structures. Failure is intended herein with reference to two different performance levels: onset of damage to non-structural elements (e.g., infills) and collapse (i.e., life-safety-threatening structural failure). However, the structures have been designed for two code-defined limit states, that is, (a) *damage-limitation* and (b) *life-safety* (except base-isolated structures which are designed for *collapse prevention*). The structures are considered as *ordinary*, that is, the reference design action are exceeded with return periods 50 years and 475 years (or 975 years for base-isolation), respectively.

For all the structures, independently of the structural typology and of the limit state, the failure rates are obtained by integration of structural fragility and seismic hazard for the sites where the structures are located. For this task equation (1), which is compliant with the performance-based earthquake engineering framework [5], is employed.

$$\lambda_f = \int_0^{+\infty} P\left[failure \middle| IM = x \right] \cdot \left| d\lambda_{IM}\left(x\right) \right| \tag{1}$$

In the equation, $\lambda_{IM}\left(x\right)$ is the annual rate of earthquake ground motions causing the

exceedance of an intensity measure (IM) when the latter equals a specific value, $IM = x$, at the building site (i.e., from probabilistic seismic hazard analysis [6]). Herein the spectral (pseudo) acceleration at the fundamental period of the structure, $Sa(T_1)$ or simply Sa, is chosen as the IM. $P[failure|IM = x]$ for different values of *x* is the fragility curve of the structure. In this study, for each designed structure, the fragility curve was computed via non-linear dynamic analysis using equation (2). To this aim, the domain of the IM has been discretized to ten values only (for which the corresponding rates of exceedance at the site has also been computed, see next section).

$$P[failure|IM = x_i] = \left\{1 - \Phi\left[\frac{\log(edp_f) - \mu_{\log(EDP|IM=x_i)}}{\sigma_{\log(EDP|IM=x_i)}}\right]\right\} \cdot \left(1 - \frac{N_{col,IM=x_i}}{N_{tot,IM=x_i}}\right) + \frac{N_{col,IM=x_i}}{N_{tot,IM=x_i}} \quad (2)$$

In the equation, EDP is a structural response measure (i.e., an engineering demand parameter); edp_f indicates structural seismic capacity for the performance level of interest; $\{\mu_{\log(EDP|IM=x_i)}, \sigma_{\log(EDP|IM=x_i)}\}$ are mean and standard deviation of the logs of EDP when $IM = x_i$, $i = \{1,\ldots,10\}$; $\Phi(\bullet)$ is the cumulative Gaussian distribution function; $N_{col,IM=x_i}$ is the number of collapse cases (i.e., those reaching global instability according the terminology in [7]); and $N_{tot,IM=x_i}$ is the number of ground motion records with $IM = x_i$, $i = \{1,\ldots,10\}$.

As discussed in the following, the method to probabilistically evaluate structural response, and then fragility, is the multi-stripe nonlinear dynamic analysis (e.g., [8]) in which ground motion input changes to reflect disaggregation of seismic hazard at the level of IM corresponding to the stripe in question; i.e., $IM = x_i$, $i = \{1,\ldots,10\}$.

3 STRUCTURES AND MODELING

The five types of buildings refer, as much as possible, to standard modern constructions and are widely representative of residential or industrial structures. Design procedures refer as much as possible to common professional engineering practice. The considered cases are briefly summarized in the following, but the interested reader should refer to the related papers for details:

1. cast-in-place reinforced concrete (RC): regular 3-, 6-, and 9-story residential moment-resisting-frame structures (bare-frames or BF, pilotis-frames or PF, infilled-frames or IF) designed via modal analysis (i.e., linear with response spectrum) [9];
2. un-reinforced masonry (URM): 2- and 3-story regular and irregular residential buildings, with four different geometries, designed with the *simple building* and *linear* or *non-linear static analysis* approaches [10];
3. pre-cast reinforced concrete (PRC): 1-story industrial buildings with two different plan geometries and two different heights [11];
4. steel (S): 1-story industrial buildings with two different plan geometries and two different heights [12];
5. base-isolated (BI): 6-story reinforced concrete residential buildings with base isolation system made of rubber bearings (HDRB), double-curvature friction pendulums (DCFP), and hybrid (HDRB and sliders) [13].

To reduce the effort, not all the structures have been designed for the five sites, although most

of them have been designed at least for three sites reflecting low, moderate and high hazard levels. Table 2 summarizes the case studies.

		MI	CL	RM	NA	AQ
RC	*Soil A*	---	---	---	---	9-story (BF/PF/IF)
	Soil C	3/6/9-story (BF/PF/IF)	6-story (BF/PF/IF)	6-story (BF/PF/IF)	3/6/9-story (BF/PF/IF) ModUnc	3/6/9-story (BF/PF/IF)
URM	*Soil A*	2/3-story, regular	2/3-story, regular	2/3-story, regular ModUnc	2/3-story, regular/irregular	2/3-story, regular ModUnc
	Soil C	2/3-story, regular	2/3-story, regular	2/3-story, regular/irregular	2/3-story, regular/irregular	2/3-story, regular/irregular
PRC	*Soil A*	1-story, geometry 1/2/3/4	---	---	1-story, geometry 1/2/3/4	1-story, geometry 1/2/3/4
	Soil C	1-story, geometry 1/2/3/4	---	---	1-story, geometry 1/2/3/4	1-story, geometry 1/2/3/4
S	*Soil A*	1-story, geometry 1/2/3/4	---	---	1-story, geometry 1/2/3/4	1-story, geometry 1/2/3/4
	Soil C	1-story, geometry 1/2/3/4	---	---	1-story, geometry 1/2/3/4	1-story, geometry 1/2/3/4
BI	*Soil A*	---	---	---	---	---
	Soil C	---	---	---	---	6-story, HDRB/HDRB+Slider/DCFP (11 configurations)

Table 2: Designed structures per site and soil category.

3D computer models were developed for all the designed structures with the aim of evaluating their seismic performance via non-linear dynamic analysis. The EDP considered is the maximum (in the two horizontal directions of the structure) demand over capacity ratio, expressed in terms of interstory drift angle or roof-drift angle (see typology-specific papers for details on capacity). All models are lumped plasticity models except for the industrial steel building cases that were modeled using distributed plasticity elements. All structures are analyzed with OPENSEES [14] with the exception of the masonry structures that have been analyzed using TREMURI [15]. All the analyses neglected, so far, the vertical components of ground motion.

In the computation of failure rates, record-to-record variability of seismic response is the primary sources of uncertainty. This means that the structural models are generally deterministic. The effect of factors, such as quality of construction or design errors, was

neglected. However, for selected cases of reinforced concrete and masonry buildings, the uncertainty in structural modeling (ModUnc) and in design has been accounted for (e.g., *within-building* variability of material characteristics and non-linear member properties [16]).[1]

4 SEISMIC HAZARD AND SEISMIC INPUT

4.1 Hazard curves

Equation (1) requires hazard curves to compute failure rates. The results of the probabilistic hazard study at the basis of NTC08 are available at http://esse1-gis.mi.ingv.it/ in terms of hazard curves for 5%-damped (pseudo) spectral acceleration on soil type A for eleven oscillation periods ranging from 0s (PGA) to 2s, computed for a grid featuring more than ten-thousands locations that covers the whole country. The curves are discretized at nine return periods between 30 years and 2,475 years. The limitation in the soil type, number of oscillation periods, and range of hazard levels of the official results forced us to re-compute the hazard curves at the five sites of interest. In addition, to underpin the record selection, disaggregation of seismic hazard [17] in terms of magnitude (M) and source-to-site distance (R) for the considered *IM*s, was also carried out.

The hazard curves were calculated according to equation (3), where ν_i, $i=\{1,2,\ldots,s\}$ is the rate of earthquakes above a minimum magnitude for each of the s seismic source zones affecting the hazard at the site of interest; $f_{M,R,i}(w,z)$ is the joint probability density function of $\{M,R\}$ of the ith zone ; and $P\left[IM>x\middle|M=w,R=z\right]$ is provided by a ground motion prediction equation (GMPE).

$$\lambda_{IM}(x)=\sum_{i=1}^{s}\nu_i\cdot\iint_{M,R}P\left[IM>x\middle|M=w,R=z\right]\cdot f_{M,R,i}(w,z)\cdot dw\cdot dz \tag{3}$$

The source model corresponding to *branch 921* of the logic tree in [2] and the GMPE of [18], that constitute the essence of the hazard model developed to produce the official seismic hazard map used for design in Italy, have been implemented in the OPENQUAKE platform [19] to fit the objectives of this study.[2] Table 3 summarizes the considered cases for which hazard curves were re-computed.

Hazard curves were discretized in ten IM values corresponding to the following return periods in years: $\{10,50,100,250,500,1000,2500,5000,10000,100000\}$. No hazard curves for return periods longer than $T_R=100000\,yr$ were calculated to avoid large extrapolations. Figure 2 shows, as an example, the curves for L'Aquila, which is the most seismically hazardous location among those considered.

Note that assessing the performance of isolated structures required considering spectral accelerations at periods longer than 2.0s. Hence, to compute hazard curves beyond that oscillation period, GMPE [21] was employed instead of GMPE [18], which is not applicable at such long periods.

[1] This activity is currently ongoing for revision and extension to other structural typologies.
[2] This combination of source model and GMPE provides hazard estimates that are close to those derived from the full logic tree [20].

Site	Soil A	Soil C
MI	$Sa(T=0.15s)$, $Sa(T=0.5s)$, $Sa(T=1.0s)$, $Sa(T=1.5s)$, $Sa(T=2.0s)$	$Sa(T=0.15s)$, $Sa(T=0.5s)$, $Sa(T=1.0s)$, $Sa(T=1.5s)$, $Sa(T=2.0s)$
CL	$Sa(T=0.15s)$, $Sa(T=0.5s)$, $Sa(T=1.5s)$	$Sa(T=0.15s)$, $Sa(T=0.5s)$, $Sa(T=1.5s)$
RM	$Sa(T=0.15s)$, $Sa(T=0.5s)$, $Sa(T=1.5s)$	$Sa(T=0.15s)$, $Sa(T=0.5s)$, $Sa(T=1.5s)$
NA	$Sa(T=0.15s)$, $Sa(T=0.5s)$, $Sa(T=1.0s)$, $Sa(T=1.5s)$, $Sa(T=2.0s)$	$Sa(T=0.15s)$, $Sa(T=0.5s)$, $Sa(T=1.0s)$, $Sa(T=1.5s)$, $Sa(T=2.0s)$
AQ	$Sa(T=0.15s)$, $Sa(T=0.5s)$, $Sa(T=1.0s)$, $Sa(T=1.5s)$, $Sa(T=2.0s)$	$Sa(T=0.15s)$, $Sa(T=0.5s)$, $Sa(T=1.0s)$, $Sa(T=1.5s)$, $Sa(T=2.0s)$, $Sa(T=3.0s)$

Table 3: Intensity measures for which hazard curves have been computed at each site.

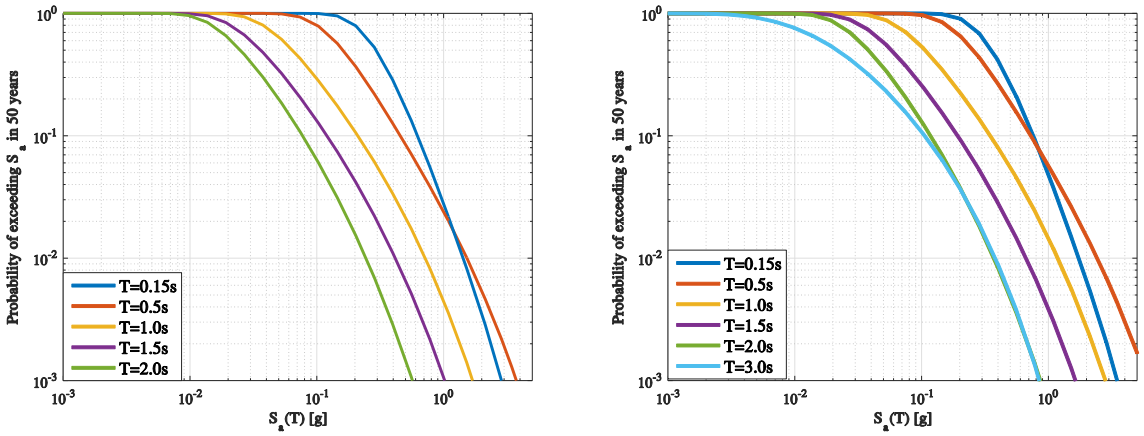

Figure 2: Hazard curves for L'Aquila for different oscillation periods on A-type soil (left) and C-type (right).

4.2 Record selection

To select the ground motion records to be used as input for dynamic analysis, the conditional spectrum (CS) approach (e.g., [22]) has been considered. The CS provides the distribution of $Sa(T)$ at any oscillation period (i.e., an elastic response spectrum) conditional on a given value of $Sa(T_1)$. In this study, ground motion record sets selected for each CS are consistent with the earthquake scenarios (expressed in terms of magnitude and source-to-site distance) that contributed the most to $Sa(T_1)=x$ at the site. Because the scenarios controlling the hazard, in general, change with the specific value of $Sa(T_1)$ considered, different sets of records were selected for each hazard level.

Records selected via the CS approach are especially suitable for non-linear dynamic multi-stripe analysis (MSA). MSA aims at computing the distributions of EDP conditional to different values of $Sa(T_1)$, here ten, as mentioned in the previous section. According to MSA, a set of response analyses is carried out for any selected level x of $Sa(T_1)$ using a suite of ground motion records scaled to have that $Sa(T_1)$ value.

An automatic procedure for record selection based on the CS approach is available at http://web.stanford.edu/~bakerjw/research/conditional_spectrum.html; its main steps can be summarized as follows: (1) definition of the distribution of $Sa(T)$ conditional on $Sa(T_1)=x$ obtained via disaggregation of seismic hazard and models for the correlation of spectral ordinates; (2) simulation of an arbitrary number of response spectra, twenty herein, consistent with the CS defined at the previous step; (3) selection of twenty records which have spectra compatible with those simulated. As an example, the records selected for L'Aquila (soil type C) for $Sa(T_1=1.0s)$, corresponding to two of the ten return periods considered, are shown in Figure 3.

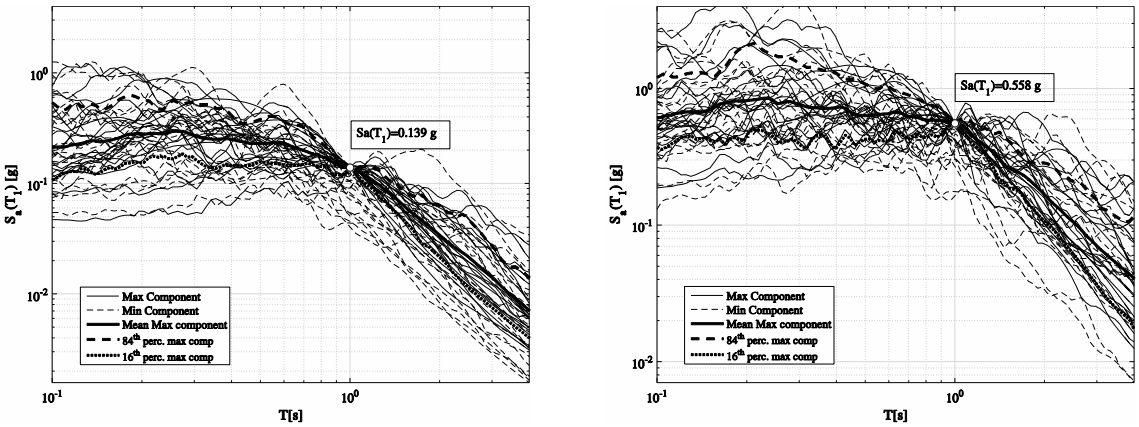

Figure 3: Spectra of selected records for L'Aquila conditional to two $Sa(T_1=1.0s)$ levels. The one corresponding to $T_R=100yr$ (left) and to $T_R=1000yr$ (right) on soil type C.

The selected records were extracted mainly from the Italian accelerometric archive (http://itaca.mi.ingv.it/; [23]) and only if no records with similar spectra were available there, suitable records in the NGAwest2 (http://peer.berkeley.edu/ngawest2/) database [24] were selected instead. Note also that, in performing step (3), the distribution of $\{M,R\}$ in each selected record set was kept consistent with the $\{M,R\}$ distribution obtained from disaggregation that was used to build the CS. This is a more refined procedure than the one adopted in standard practice that considers matching the CS as the only requirement for the record selection.

Note that to be consistent with GMPE [18], which has been developed for the maximum horizontal component, the matching of the CS has been done utilizing the horizontal component with the maximum value of the conditioning IM. Conversely, for those cases where the GMPE of [21] was considered, the CS matching was executed using the geometric mean of the two horizontal components.

The record selection delivered two-hundreds pairs of records for each IM, twenty records for each one of the ten stripes. It means that two-hundred records have been employed in the

analysis of each individual structure. To reduce the computational demand from non-linear dynamic analysis, the selected records have been post processed to remove the parts of the signal outside $\{t_{0.05\%}, t_{99.95\%}\}$ range, where $D_{99.90\%} = t_{99.95\%} - t_{0.05\%}$ is the 99.90% bracketed duration of the record [25], yet keeping synchronization of horizontal components.

5 RESULTS AND DISCUSSIONS

5.1 Risk assessment

Equation (1) can be used for the computation of failure rates only for the values of $\lambda_{IM}(x)$ provided by hazard analysis, the latter, as discussed, has limit at $T_R = 100000\,yr$. Therefore, it has been conservatively assumed that ground motions with an IM larger than that corresponding to $T_R = 100000\,yr$, called here $IM_{T_R^*}$, cause failure with certainty. This means that the failure rate has been approximated in excess by:

$$\begin{aligned}\lambda_f &= \int_0^{IM_{T_R^*}} P\left[failure \middle| IM = x\right] \cdot \left|d\lambda_{IM}(x)\right| + \int_{IM_{T_R^*}}^{+\infty} 1 \cdot \left|d\lambda_{IM}(x)\right| \\ &= \int_0^{IM_{T_R^*}} P\left[failure \middle| IM = x\right] \cdot \left|d\lambda_{IM}(x)\right| + 10^{-5}\end{aligned} \tag{4}$$

In those cases, when the first part of the integral is negligible with respect to 10^{-5}, then equation (4) only allows to state that the annual failure rate lower than 10^{-5}.

5.2 Site-to-site and structure-to-structure risk variations

Figure 4 and Figure 5 give an overview of the annual failure rates associated to collapse. Each figure refers to one soil condition and the markers refer to the different structures reported in Table 2.

Data are ordered by increasing hazard of the corresponding site (see Table 1). Markers that are on a horizontal stripe and not vertically aligned on each site are spread only for readability. The failure rates equal to 10^{-5} correspond to cases where the hazard beyond IM_{TR*} dominates the risk, and 10^{-5} is an upper bound of the actual failure rate.

The main preliminary results emerging from the computed failure rates are that, generally, seismic risk of code-conforming structures tends to increase with the hazard level of the building site. Moreover, the failure rate is below 10^{-5} in many cases for low and moderate hazard locations (especially for reinforced-concrete structures), which may be an effect of minimum design requirements of the code. The risk is not uniform among different structure types designed for the same site, which may also be an effect of the diverse design procedures adopted in standard practice for different building types. Base-isolated buildings seem to have a collapse failure rate larger than that of other building types (note that the rates of exceeding the onset of non-structural damage in base-isolated structures, not shown herein, is instead significantly lower).

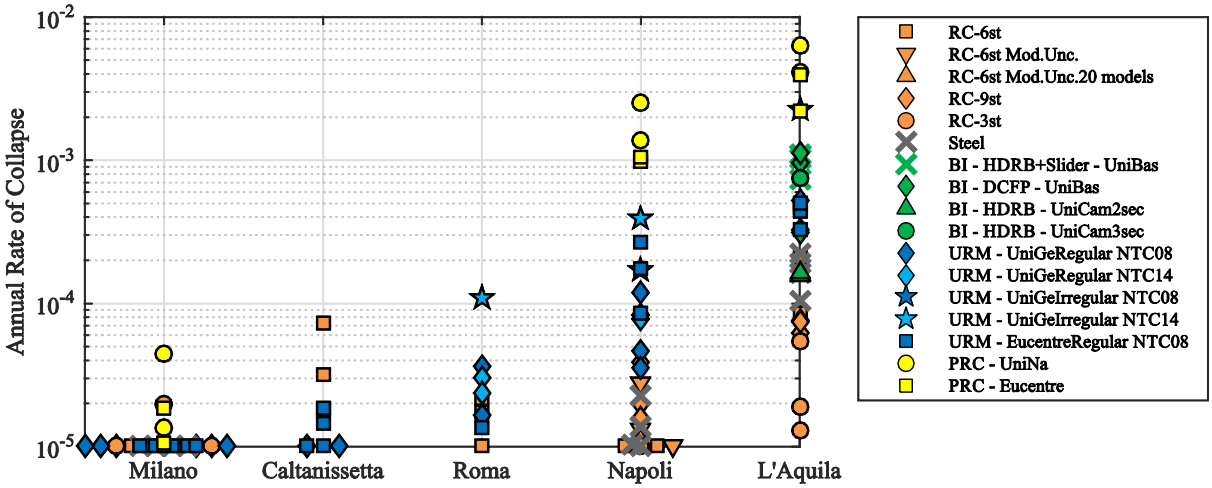

Figure 4: Annual failure (collapse) rates (soil C-type).

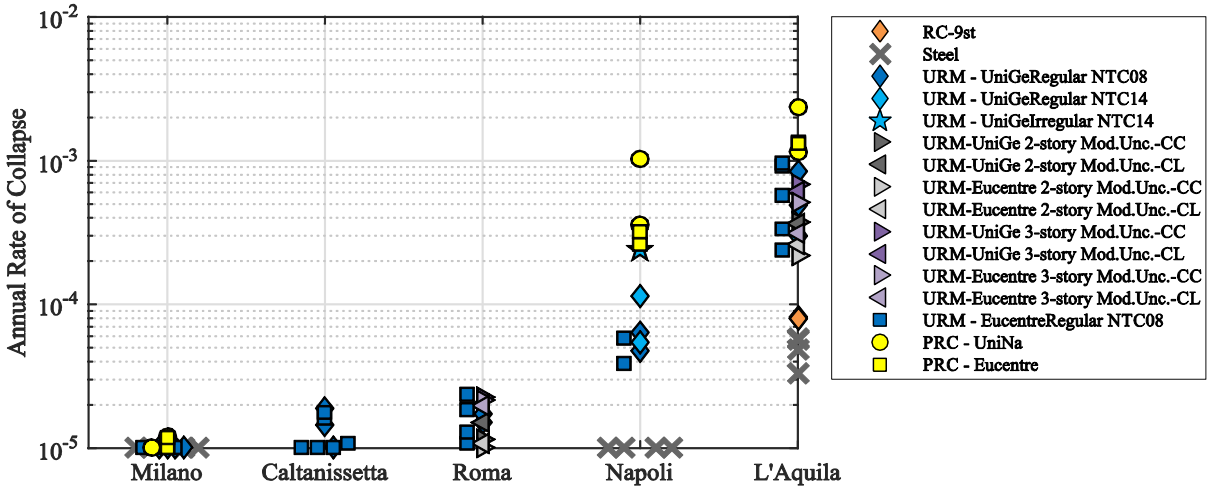

Figure 5: Annual failure (collapse) rates (soil A-type).

6 CONCLUSIONS

This paper briefly presented the failure (collapse) rates for a set of structures belonging to the most common types in Italy. These structures were designed for life-safety (or collapse prevention) for several sites characterized by diverse seismicity levels and for two soil conditions. Nonlinear dynamic analysis, in the form of multiple stripe analysis, was the method chosen to perform structural fragility assessment for two damage states: onset of damage and collapse. The fragility curves were coupled with the site hazard curves to compute the annual failure rates for both damage states. However, only collapse failure rates were shown. The uncertainty was accounted in the hazard, in the record-to-record variability of structural response, and, for a few cases, also in the structural modeling. The preliminary results of the first two years of the project indicate the following:

1. in some cases, the collapse failure rates are so low that only an upper bound to the actual failure rate can be provided; i.e., $\lambda_f \leq 10^{-5}$;
2. the collapse failure rates tend to increase with the site hazard;
3. the collapse failure rates are also not uniform among different building types designed for the same site;
4. the collapse failure rates of buildings at the most hazardous of the sites exceed 10^{-5} for all structural types and, in some cases, are comparable to the annual rate of exceedance of the design seismic intensity;

5. the comparatively high collapse failure rates of base-isolated structure may be due to their more controlled behavior during design and the lower margin of safety with respect to collapse beyond the maximum design displacement; conversely, base-isolated structures show comparatively lower onset of damage failure rates, (not shown herein);
6. failure rates for onset of non-structural damage (not shown herein) show a general trend similar to the collapse failure rates discussed here.

It is emphasized that the project is still ongoing and several of these results (and other not exhibited here) are undergoing verification and investigation. Caution should be applied in using all results presented; in particular, those related to some RC buildings, base-isolated structures, steel and pre-cast concrete industrial structures, as well as some masonry buildings, before the final verification is over. The results discussed here are not final and might be subject to significant updates at the end of the project.

7 ACKNOWLEDGMENTS

The study was developed between 2015 and 2016 in the framework the ReLUIS-DPC and EUCENTRE-DPC projects, funded by the Italian civil protection (DPC). The following universities, beyond those of the affiliation of the authors, participated to the project for design, modeling and analysis of the structures for which the failure rates were computed, in random order: *Sapienza Università di Roma*, *Università di Chieti-Pescara G. D'Annunzio*, *Università degli Studi della Basilicata*, *Università degli Studi di Camerino*, *Università degli Studi di Padova*, *Università degli Studi di Genova*. We also gratefully acknowledged the contribution of Emilia Fiorini for the computation of the hazard curves for Italy.

8 REFERENCES

[1] CS.LL.PP. DM 14 Gennaio, Norme tecniche per le costruzioni, *Gazzetta Ufficiale della Repubblica Italiana* **29**, 2008. (in Italian)

[2] M. Stucchi, C. Meletti, V. Montaldo, H. Crowley, G.M. Calvi, E. Boschi, Seismic hazard assessment (2003–2009) for the Italian building code. *B. Seismol. Soc. Am.*, **101**, 1885-1911, 2011.

[3] CEN, European Committee for Standardisation TC250/SC8/ *Eurocode 8: Design Provisions for Earthquake Resistance of Structures, Part 1.1: General rules, seismic actions and rules for buildings*, PrEN1998-1, 2003.

[4] RINTC Workgroup, *Results of the 2015-2016 RINTC project*. ReLUIS report, ReLUIS, Naples, Italy, 2017. Available at http://www.reluis.it/

[5] C.A. Cornell, H. Krawinkler, Progress and challenges in seismic performance assessment, *PEER Center News* 3, 1-3, 2000.

[6] C.A. Cornell, Engineering seismic risk analysis, *B. Seismol. Soc. Am.* **58**, 1583-1606, 1968.

[7] N. Shome, C.A. Cornell, Structural seismic demand analysis: Consideration of "Collapse", *PMC2000 - 8th ASCE Specialty Conference on Probabilistic Mechanics and Structural Reliability*. University of Notre Dame, South Bend, Indiana, 24-26 July, 2000.

[8] F. Jalayer, *Direct probabilistic seismic analysis: implementing non-linear dynamic assessments*, Ph.D. thesis, Stanford University, California, 2003.

[9] G. Camata, F. Celano, M.T. De Risi, P. Franchin, G. Magliulo, V. Manfredi, A. Masi, F.

Mollaioli, F. Noto, P. Ricci, E. Spacone, M. Terrenzi, G. Verderame, RINTC project: Nonlinear Dynamic Analyses of Italian code-conforming Reinforced Concrete Buildings for Risk of Collapse Assessment, *COMPDYN 2017 - 6th ECCOMAS Thematic Conference on Computational Methods in Structural Dynamics and Earth-quake Engineering*, M. Papadrakakis, M. Fragiadakis (eds.) Rhodes Island, Greece, 15–17 June 2017.

[10] D. Camilletti, S. Cattari, S. Lagomarsino, D. Bonaldo, G. Guidi, S. Bracchi, A. Galasco, G. Magenes, C.F. Manzini, A. Penna, M. Rota, RINTC project: Nonlinear dynamic analyses of Italian code-conforming URM buildings for collapse risk assessment, *COMPDYN 2017 - 6th ECCOMAS Thematic Conference on Computational Methods in Structural Dynamics and Earthquake Engineering*, M. Papadrakakis, M. Fragiadakis (eds.), Rhodes Island, Greece, 15–17 June 2017.

[11] M. Ercolino, M. Cimmino, G. Magliulo, D. Bellotti, R. Nascimbene, RINTC project: Nonlinear analyses of Italian code conforming precast R/C industrial buildings for risk of collapse assessment, *COMPDYN 2017 - 6th ECCOMAS Thematic Conference on Computational Methods in Structural Dynamics and Earthquake Engineering*, M. Papadrakakis, M. Fragiadakis (eds.), Rhodes Island, Greece, 15–17 June 2017.

[12] F. Scozzese, G. Terracciano, A. Zona, G. Della Corte, A. Dall'Asta, R. Landolfo, RINTC project: Nonlinear dynamic analyses of Italian code-conforming steel single-story buildings for collapse risk assessment, *COMPDYN 2017 - 6th ECCOMAS Thematic Conference on Computational Methods in Structural Dynamics and Earth-quake Engineering*, M. Papadrakakis, M. Fragiadakis (eds.) Rhodes Island, Greece, 15–17 June 2017.

[13] F.C. Ponzo, D. Cardone, A. Dall'Asta, A. Di Cesare, G. Leccese, A. Mossucca, N. Conte, A. Flora, L. Ragni**,** F. Micozzi, RINTC project: Nonlinear analyses of Italian code-conforming base-isolated buildings for risk of collapse assessment, *COMPDYN 2017 - 6th ECCOMAS Thematic Conference on Computational Methods in Structural Dynamics and Earthquake Engineering*, M. Papadrakakis, M. Fragiadakis (eds.) Rhodes Island, Greece, 15–17 June 2017.

[14] S. Mazzoni, F. McKenna, M.H. Scott, G.L. Fenves. *OpenSees Command Language Manual*. Pacific Earthquake Engineering Research (PEER) Center, Berkeley, California, 2006. Available at http://opensees.berkeley.edu/

[15] S. Lagomarsino, A. Penna, A. Galasco, S. Cattari. TREMURI program: an equivalent frame model for the nonlinear seismic analysis of masonry buildings, *Eng. Struct.*, **56**, 1787-1799, 2013.

[16] P. Franchin, F. Mollaioli, F. Noto, RINTC project: Influence of structure-related uncertainties on the risk of collapse of Italian code-conforming reinforced concrete buildings, *COMPDYN 2017 - 6th ECCOMAS Thematic Conference on Computational Methods in Structural Dynamics and Earthquake Engineering*, M. Papadrakakis, M. Fragiadakis (eds.) Rhodes Island, Greece, 15–17 June 2017.

[17] P. Bazzurro, C.A. Cornell, Disaggregation of seismic hazard, *B. Seismol. Soc. Am.,* **89**, 501-520, 1999.

[18] N.N. Ambraseys, K.U. Simpson, J.J. Bommer, Prediction of horizontal response spectra in Europe, *Earthq. Eng. Struct. D.*, **25**, 371-400, 1996.

[19] D. Monelli, M. Pagani, G. Weatherill, V. Silva, H. Crowley, The hazard component of OpenQuake: The calculation engine of the Global Earthquake Model. *15WCEE - 15th world conference on earthquake engineering*, Lisbon, Portugal, 24–25 September 2012.

[20] S. Barani, D. Spallarossa, P. Bazzurro, Disaggregation of probabilistic ground-motion hazard in Italy, *B. Seismol. Soc. Am.*, **99**, 2638-2661, 2009.

[21] S. Akkar, J.J. Bommer, Empirical Equations for the Prediction of PGA, PGV, and Spectral Accelerations in Europe, the Mediterranean Region, and the Middle East, *Seismol. Res. Lett.*, **81**, 195-206, 2010.

[22] T. Lin, C.B. Haselton, J.W. Baker, Conditional spectrum-based ground motion selection. Part I: Hazard consistency for risk-based assessments, *Earthq. Eng. Struct. D.*, **42**, 1847-1865, 2013.

[23] L. Luzi, S. Hailemikael, D. Bindi, F. Pacor, F. Mele, F. Sabetta, ITACA (ITalian ACcelerometric Archive): a web portal for the dissemination of Italian strong-motion data, *Seismol. Res. Lett.,* **79**, 716-722, 2008.

[24] T.D. Ancheta, R.B. Darragh, J.P. Stewart, et al., NGA-West2 database, *Earthq. Spectra*, **30**, 989-1005.

[25] R. Dobry, I.M. Idriss, E. Ng, Duration characteristics of horizontal components of strong-motion earthquake records. *B. Seismol. Soc. Am.*, 68, 1487-1520, 1978.